BIOCHEMISTRY
including biophysical chemistry & molecular biology

Article

pubs.acs.org/biochemistry

Recognition of Heteropolysaccharide Alginate by Periplasmic Solute-Binding Proteins of a Bacterial ABC Transporter

Yu Nishitani,[†] Yukie Maruyama,[†] Takafumi Itoh,[†] Bunzo Mikami,[‡] Wataru Hashimoto,[†] and Kousaku Murata*[,†]

[†]Laboratory of Basic and Applied Molecular Biotechnology, Graduate School of Agriculture, Kyoto University, Uji, Kyoto 611-0011, Japan

[‡]Laboratory of Applied Structural Biology, Graduate School of Agriculture, Kyoto University, Uji, Kyoto 611-0011, Japan

Supporting Information

ABSTRACT: Alginate is a heteropolysaccharide that consists of β-D-mannuronate (M) and α-L-guluronate (G). The Gram-negative bacterium *Sphingomonas* sp. A1 directly incorporates alginate into the cytoplasm through the periplasmic solute-binding protein (AlgQ1 and AlgQ2)-dependent ABC transporter (AlgM1-AlgM2/AlgS-AlgS). Two binding proteins with at least four subsites strongly recognize the nonreducing terminal residue of alginate at subsite 1. Here, we show the broad substrate preference of strain A1 solute-binding proteins for M and G present in alginate and demonstrate the structural determinants in binding proteins for heteropolysaccharide recognition through X-ray crystallography of four AlgQ1 structures in complex with saturated and unsaturated alginate oligosaccharides. Alginates with different M/G ratios were assimilated by strain A1 cells and bound to AlgQ1 and AlgQ2. Crystal structures of oligosaccharide-bound forms revealed that in addition to interaction between AlgQ1 and unsaturated oligosaccharides, the binding protein binds through hydrogen bonds to the C4 hydroxyl group of the saturated nonreducing terminal residue at subsite 1. The M residue of saturated oligosaccharides is predominantly accommodated at subsite 1 because of the strict binding of Ser-273 to the carboxyl group of the residue. In unsaturated trisaccharide (ΔGGG or ΔMMM)-bound AlgQ1, the protein interacts appropriately with substrate hydroxyl groups at subsites 2 and 3 to accommodate M or G, while substrate carboxyl groups are strictly recognized by the specific residues Tyr-129 at subsite 2 and Lys-22 at subsite 3. Because of this substrate recognition mechanism, strain A1 solute-binding proteins can bind heteropolysaccharide alginate with different M/G ratios.

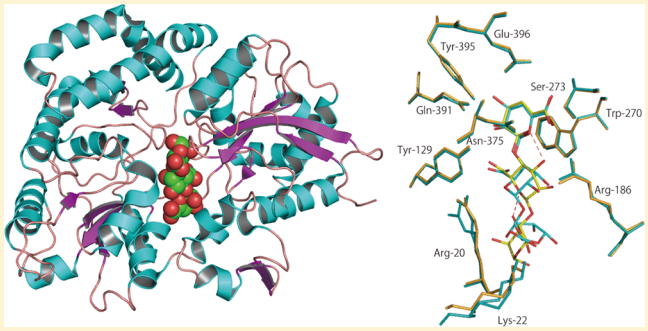

Alginate is an acidic heteropolysaccharide that consists of β-D-mannuronate (M) and the C5 epimer α-L-guluronate (G).[1] The alginate polymer consists of poly(M), poly(G), and heteropolymeric random sequences poly(MG). Because of their different configurations, poly(M) adopts a linear extended conformation, whereas poly(G) exhibits a buckled structure. Brown seaweeds and certain bacteria are known to produce alginate.[2] Seaweed alginate is widely used as a gelling agent in food, pharmaceutical, cosmetic, and medical industries, and enzymatically degraded oligosaccharides show potent physiological activity as elicitors in plants and bifidobacteria.[3] On the other hand, *Pseudomonas* alginate functions as a biofilm involved in bacterial respiratory infectious diseases, particularly in cystic fibrosis patients.[4] A large number of reports on alginate-degrading microbes and/or enzymes have been published, providing useful biochemicals for modifying or processing edible seaweed alginate and removing bacterial biofilm alginate.[5]

The use of sugar cane and corn starch for the production of ethanol has produced serious social problems, such as their insufficient supply and the sudden increase in prices.[6] Recently, marine biomass has been recognized as a promising source for biofuel production. Brown seaweed, a type of marine biomass, can be readily cultivated and has not been exploited as a major crop. Alginate is an attractive marine biomass component because of its high content (30−60%) in dried seaweeds and easy extraction; the M/G ratio in alginate varies depending on the producer species, season, and area.[7] Nevertheless, in comparison to neutral starch and cellulose in land plants, little information about the utilization of this acidic polysaccharide is available.

In general, microbes secrete polysaccharide-degrading enzymes extracellularly and incorporate degraded oligosaccharides into microbial cells when grown on polysaccharides. This mechanism is considered to be an extracellular degrading enzyme-dependent assimilation system. In particular, polysaccharide lyases are key enzymes for microbial degradation of acidic polysaccharides such as alginate and pectin.[8] On the

Received: February 10, 2012
Revised: April 5, 2012
Published: April 9, 2012

other hand, the Gram-negative *Sphingomonas* sp. A1 (strain A1) isolated from a paddy field as an alginate-assimilating bacterium is peculiar in that the bacterium directly incorporates external alginate into the cytoplasm simultaneously across the outer and inner membranes and degrades the polysaccharide by cytoplasmic alginate lyases.[9] The alginate incorporation machinery of strain A1 includes three component segments: a pit on the cell surface,[10] solute-binding proteins in the periplasm,[11] and an ATP-binding cassette (ABC) transporter in the inner membrane.[12] The cell surface pit with a diameter of 0.02−0.1 μm is formed to accumulate external alginate through rearrangement of pleat molecules. Periplasmic alginate-binding proteins (AlgQ1 and AlgQ2) mediate the transfer of the polysaccharide from the cell surface to the inner membrane. The inner membrane-bound ABC transporter (AlgM1-AlgM2/AlgS-AlgS) directly incorporates alginate into the cytoplasm with the energy generated through ATP hydrolysis. Heterodimeric membrane proteins AlgM1-AlgM2 and homodimeric ATPase (AlgS-AlgS) constitute the ABC transporter. Incorporated alginate is then depolymerized into di-, tri-, and tetrasaccharides through the action of three cytoplasmic endotype alginate lyases, namely, A1-I, A1-II, and A1-III.[13] The alginate oligosaccharides thus formed are finally degraded into monosaccharides by cytoplasmic exotype alginate lyase A1-IV with a broad substrate preference for M and G.[14] Distinct from ordinary bacterial solute-binding protein-dependent ABC transporters,[15] the strain A1 uptake system is characteristic in that the substrate is a macromolecule. This is the first identified alginate import system, although pectin assimilation mechanisms, including extracellular degradation, import of oligosaccharide across the membrane, and monosaccharide metabolism, have been well documented in the plant pathogenic bacteria *Erwinia chrysanthemi*.[16]

Because substrate recognition by solute-binding proteins triggers import by ABC transporters, binding of AlgQ1 and AlgQ2 to heteropolysaccharide alginate is crucial for the macromolecule import mechanism. The two alginate-binding proteins, AlgQ1 and AlgQ2, resemble each other in primary structure and specifically bind and release alginate macromolecules, respectively.[17] X-ray crystallography has revealed that both proteins composed of N- and C-domains bind alginate in the deep cleft formed when the N- and C-domains close and release the polymer when the domains open.[11,18] Positively charged residues in the active cleft allow AlgQ1 and AlgQ2 to bind acidic alginate preferentially. Although the proteins tightly bind the nonreducing terminal residues of alginate molecules, at least four subsites that accommodate sugar residues are present in the active cleft. Recognition of heteropolysaccharide alginate by these binding proteins, however, remains to be clarified. More recently, genetically engineered strain A1 cells with an ethanol fermenting ability have been shown to produce ethanol from alginate.[19] The recognition mechanism of AlgQ1 and AlgQ2 for M and G present in alginate molecules is also important for effective import and utilization of the marine biomass in strain A1 cells. This article addresses the mode of binding of AlgQ1 to M and G at each subsite through the determination of crystal structures in complex with alginate oligosaccharides with different M/G ratios.

MATERIALS AND METHODS

Bacterial Culture. To investigate the preference for M, G, or both in alginate, strain A1 cells were aerobically cultured at 30 °C in an alginate medium consisting of 0.1% $(NH_4)_2SO_4$, 0.1% KH_2PO_4, 0.1% Na_2HPO_4, 0.01% $MgSO_4{\cdot}7H_2O$, 0.01% yeast extract, and 0.5% sodium alginate (pH 7.2). Four types of sodium alginate were used. *Eisenia bicyclis* sodium alginate (M/G ratio of 56.5/43.5) was purchased from Nacalai Tesque. Three kinds of sodium alginate, I-1 (M/G ratio of 56.5/43.5), I-1G (M/G ratio of 41.2/58.8), and I-1 M (M/G ratio of 73.3/26.7), were kind gifts from Kimica. The turbidity of the culture was periodically measured at 600 nm.

Protein Expression and Purification. *Escherichia coli* strain HMS174(DE3)pLysS (Novagen) was used as the host for the expression of AlgQ1.[17] For expression in *E. coli*, the cells were aerobically precultured at 30 °C in Luria-Bertani medium[20] supplemented with sodium ampicillin (0.1 mg/mL). When the turbidity reached approximately 0.5 at 600 nm, isopropyl β-D-thiogalactopyranoside was added to the culture (0.1 mM), and the cells were further cultured at 16 °C for 44 h. Unless otherwise specified, all operations were performed at 0−4 °C. *E. coli* cells harboring plasmid pAQ1[17] were grown in 6 L of LB medium (1.5 L/flask), collected by centrifugation at 6000*g* and 4 °C for 5 min, washed with 20 mM potassium phosphate buffer (pH 7.0), and resuspended in the same buffer. The cells were ultrasonically disrupted (Insonator model 201M, Kubota) at 0 °C and 9 kHz for 20 min, and the clear solution obtained after centrifugation at 20000*g* and 4 °C for 20 min was used as the cell extract. AlgQ1 was purified from the cell extract by cation-exchange chromatography [CM-Toyopearl 650 M column (2.6 cm × 20 cm) (Tosoh)] and gel filtration chromatography [Sephacryl S-200 HR column (2.6 cm × 100 cm) (GE Healthcare)]. The eluted protein AlgQ1 was dialyzed against 20 mM Tris-HCl (pH 7.5) overnight. The dialysate was used as purified AlgQ1. Expression and purification of AlgQ2 were conducted as described previously.[11] The homogeneity of the purified protein was confirmed by sodium dodecyl sulfate−polyacrylamide gel electrophoresis.[21]

Preparation of Alginate Derivatives. M- and G-rich saccharides were separated from seaweed alginate as described previously, but with slight modifications.[22] *E. bicyclis* sodium alginate (10 g) was hydrolyzed at 100 °C for 90 min with 0.3 M HCl (1 L). After acid hydrolysis, the reaction mixture was subjected to centrifugation at 1650*g* and 25 °C for 20 min, and the resultant precipitant saccharides were washed with 0.3 M HCl and resuspended in distilled water (125 mL). After solubilization by neutralization with NaOH, saccharides were concentrated and dried by centrifugation under vacuum. The resultant saccharides were dissolved in 0.1 M NaCl (250 mL), and the solution was adjusted to pH 2.85 with 30 mM HCl (250 mL). After centrifugation at 1650*g* and 25 °C for 20 min, the reaction mixture was separated into G-rich saccharides as the precipitant and M-rich saccharides as the supernatant. The precipitant was washed with 0.1 M HCl (100 mL) and resuspended in distilled water (150 mL), followed by solubilization by adjustment at pH 7.0 with NaOH. The G-rich saccharides were precipitated with ethanol (300 mL) and freeze-dried after being washed twice with ethanol and centrifugation. The resultant powder was used as G-rich saccharides. The supernatant (500 mL) containing M-rich saccharides was adjusted to pH 7.0 with NaOH and treated with ethanol (1 L). The precipitated M-rich saccharides were freeze-dried after being washed twice with ethanol. The resultant powder was used as M-rich saccharides. M- and G-rich saccharides were subjected to nuclear magnetic resonance (NMR) analysis to determine the content of M and G.

dx.doi.org/10.1021/bi300194f | *Biochemistry* 2012, 51, 3622−3633

Saturated alginate oligosaccharides were prepared as follows. M-Rich saccharides (0.3% solution) were hydrolyzed at 100 °C for 20 h with 7 mM HCl. After neutralization with NaOH, the hydrolysates were concentrated by being freeze-dried and subjected to gel filtration chromatography [Biogel P-6 column (1.5 cm × 140 cm) (Bio-Rad)]. Each saturated monosaccharide (M), disaccharide (MM), and trisaccharide (MMM) was purified to homogeneity. Similarly, the saturated monosaccharide (G), disaccharide (GG), and trisaccharide (GGG) were purified from G-rich saccharides by acid hydrolysis and gel filtration.

Unsaturated alginate oligosaccharides were prepared by treatment with alginate lyase. M-Rich saccharides (10%) in 20 mM Tris-HCl (pH 7.5) were incubated at 25 °C for 12 h with alginate lyase A1-III[13] specific for M-rich saccharides. Enzymatically degraded saccharides were subjected to anion-exchange chromatography [Q-Sepharose HP column (2.6 cm × 10 cm) (GE healthcare)] and eluted with a linear gradient of an ammonium bicarbonate solution. Unsaturated disaccharide (ΔMM) and trisaccharide (ΔMMM) were purified to homogeneity. Similarly, alginate lyase A1-II′[23] capable of degrading G-rich saccharides was used for the preparation of unsaturated disaccharide (ΔGG) and trisaccharide (ΔGGG).

The homogeneity of oligosaccharides was confirmed by thin-layer chromatography as described previously.[14]

NMR. M- and G-rich saccharides were lyophilized and dissolved in deuterium oxide. ^{1}H NMR spectral analysis of the saccharides was performed at 400 MHz with a Bruker AV400M instrument provided by Hitachi Chemical Techno Service.

Sugar Assay. The concentration of alginate oligosaccharides was measured with glucose as the standard according to the dinitrosalicylic acid method[24] based on the determination of reducing sugars.

Differential Scanning Fluorimetry (DSF). Interaction between solute-binding proteins (AlgQ1 and AlgQ2) and alginate oligosaccharides (MMM, GGG, ΔMMM, and ΔGGG) was assessed by DSF as described by Niesen et al.[25] In brief, this method was performed using the MyiQ2 real-time polymerase chain reaction (PCR) instrument (Bio-Rad). The fluorescence of SYPRO Orange (Invitrogen) was monitored using filters provided with the PCR instrument (excitation at 492 nm and emission at 610 nm). The reaction mixture (20 μL) consisting of AlgQ1 or AlgQ2 (1.7 μM), each oligosaccharide (0, 1, 2, 4, 8, 16, 32, 64, 128, 256, or 512 μM), SYPRO Orange (1000-fold diluted), and Tris-HCl (20 mM, pH 7.5) was subjected to heat treatment. The temperature was increased from 25 to 95 °C by 0.5 °C/cycle (10 s/cycle) for a total of 141 cycles. The fluorescence emitted from SYPRO Orange upon binding to the denatured protein was measured. The fluorescence profile was obtained by plotting the relative fluorescence unit (RFU) at every temperature. The resultant fluorescence profile was analyzed using *iQ5* (Bio-Rad), and the midpoint of the increase in the profile was defined as the melting temperature (T_m).

Crystallization and X-ray Diffraction. Purified AlgQ1 was concentrated by ultrafiltration using Centriprep (10000 molecular weight cutoff) (Millipore) to 15 mg/mL. The protein crystals in complex with MMM, MG, and ΔMMM were prepared at 20 °C by hanging-drop vapor diffusion; the reservoir solution for the AlgQ1-MMM or AlgQ1-MG crystal consisted of 20% (w/v) polyethylene glycol 10000 and 0.1 M 4-(2-hydroxyethyl)-1-piperazineethanesulfonic acid (pH 7.5). In the case of AlgQ1-ΔMMM crystals, the reservoir solution included 20% (w/v) polyethylene glycol 4000 and 0.1 M sodium citrate (pH 5.6). The 3 μL of protein solution containing each alginate oligosaccharide (MMM, GG, or ΔMMM) at 1 mM was mixed with an equal volume of a reservoir solution. Distinct from the aforementioned crystals, AlgQ1 in complex with ΔGGG was crystallized at 20 °C by sitting-drop vapor diffusion against 20% (w/v) polyethylene glycol 10000 and 0.1 M 4-(2-hydroxyethyl)-1-piperazineethanesulfonic acid (pH 7.5). The 1 μL of protein solution containing 1 mM ΔGGG was mixed with an equal volume of the reservoir solution. Crystals were placed in a cold nitrogen gas stream at −173 °C. X-ray diffraction images were collected using a Quantum 315 charge-coupled device detector (ADSC) for AlgQ1-MMM, AlgQ1-MG, and AlgQ1-ΔGGG crystals or a Jupiter 210 charge-coupled device detector (Rigaku) for AlgQ1-ΔMMM crystals, with synchrotron radiation at a wavelength of 1.00 Å at the BL-38B1 station of SPring-8 (Hyogo, Japan). The data were processed and scaled using *HKL2000*.[26]

Structure Determination and Refinement. The structure of AlgQ1-ΔMMM was determined through molecular replacement with *CNS*[27] using previously determined coordinates of AlgQ1-ΔMM [Protein Data Bank (PDB) entry 1Y3N] as an initial model and refined with *ShelXL*.[28] Other structures of AlgQ1-MMM, AlgQ1-MG, and AlgQ1-ΔGGG were determined through molecular replacement with *Molrep*[29] supplied in the *CCP4 interface* program package[30] using coordinates of AlgQ1-ΔMMM as an initial model. Structure refinement was conducted using *Refmac5*.[31] Randomly selected reflections (5%) were excluded from refinement and were used to calculate R_{free}. After each refinement cycle, the model was adjusted manually using *winCoot*.[32] Water molecules were incorporated where the difference in density exceeded 3.0σ above the mean, and the $2F_o - F_c$ map showed a density of more than 1.0σ. Alginate oligosaccharide parameter files for structure refinement were constructed at the PRODRG site.[33] Protein models were superimposed, and their root-mean-square deviation (rmsd) was determined with *LSQKAB*,[34] part of the *CCP4* program package. Final model quality was checked with *PROCHECK*,[35] and a cis peptide bond was observed at Pro-312. Figures for protein structures were prepared using *PyMOL*.[36] Coordinates used in this work were taken from the PDB of the Research Collaboratory for Structural Bioinformatics.[37]

Accession Numbers. The atomic coordinates and structure factors for AlgQ1-ΔMMM (entry 3A09), AlgQ1-ΔGGG (entry 3VLV), AlgQ1-MMM (entry 3VLU), and AlgQ1-MG (entry 3VLW) have been deposited in the PDB.

RESULTS AND DISCUSSION

Growth of Strain A1. Because alginate contains both M and G residues, three block regions (M-rich, G-rich, and randomly sequenced residues) are included in the molecule. To examine the preference of strain A1 for M, G, or both, the growth of strain A1 cells was periodically determined by measuring the turbidity of the culture. Although sodium alginate purchased from Nacalai Tesque and sodium alginate I-1 obtained from Kimica show identical M/G ratios (56.5/43.5), there is a significant difference in molecular mass between them. Nacalai alginate has a higher molecular mass than Kimica alginate I-1. The viscosity of 1% of each alginate solution at 20 °C is as follows: Nacalai alginate, 1000 mPa/s; Kimica alginate I-1, 100−200 mPa/s. Although the slight difference in the

growth curve of strain A1 on Nacalai alginate and Kimica alginate I-1 was observed probably due to the molecular mass or molar concentration of both polymers, no significant difference was found in the growth of strain A1 among four types of alginate with different M/G ratios in the media tested (Figure 1). This result suggests that alginate import proteins of

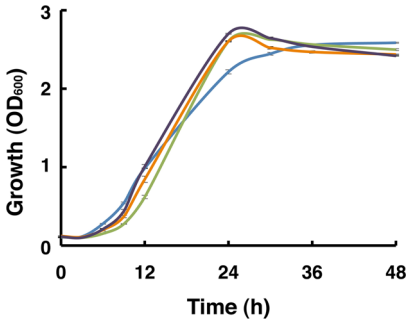

Figure 1. Strain A1 cells were grown on various alginates with different M/G ratios: orange for I-1G (41.2/58.8), violet for I-1 (56.5/43.5), green for I-1M (73.3/26.7), and blue for sodium alginate (56.5/43.5). Although sodium alginate purchased from Nacalai and sodium alginate I-1 obtained from Kimica show identical M/G ratios (56.5/43.5), there is a significant difference in molecular mass between them. This growth experiment was conducted thrice.

strain A1 show an ability to interact with both M and G residues. Hereafter, the focus will be on the recognition mechanism of heteropolyaccharide alginate by the periplasmic solute-binding proteins, AlgQ1 and AlgQ2.

Affinity of AlgQ1 and AlgQ2 for Alginate Oligosaccharides. To prepare various alginate oligosaccharides, saturated and unsaturated oligosaccharides (mono-, di-, and trisaccharides) were obtained from M- and G-rich saccharides by acid hydrolysis and lyase treatment, respectively. Saturated and unsaturated trisaccharides obtained from M-rich saccharides were designated as MMM and ΔMMM, respectively. Similarly, GGG and ΔGGG are trisaccharides obtained from G-rich saccharides. The composition of these saccharides was determined using ^{1}H NMR analysis (Figure 2). More than 90% of G residues were present in G-rich saccharides, whereas only 72% of M residues were present in M-rich saccharides.

The affinity of AlgQ1 and AlgQ2 for alginate oligosaccharides was inferred using DSF[25] on the basis of changes in protein stability by ligand binding. This method has already been adopted to study the interaction between bacterial periplasmic solute-binding proteins and substrate ligands.[38] Four alginate trisaccharides (MMM, ΔMMM, GGG, and ΔGGG) were used as substrate ligands in this experiment. The fluorescence of SYPRO Orange that bound to denatured proteins was measured during heat treatment (from 25 to 95 °C). Melting temperatures (T_m) of AlgQ1 and AlgQ2 in the absence and presence of trisaccharides were determined as the midpoint of the increase in the fluorescence profile (Table 1). For example, the fluorescence profile of AlgQ1 in the presence of the dye shifted to a higher temperature in proportion to the increase in the concentration of MMM added (Figure 3, top), suggesting that the ligand-bound AlgQ1 was thermally more stable than the ligand-free protein. On the other hand, there was no difference in the T_m values of alginate-binding proteins in the absence or presence of cellotriose (data not shown). Almost a single midpoint (T_m, 51.3 °C) was observed in the profile of AlgQ1 in absence of MMM; two T_m values (52.5 and 57.6 °C)

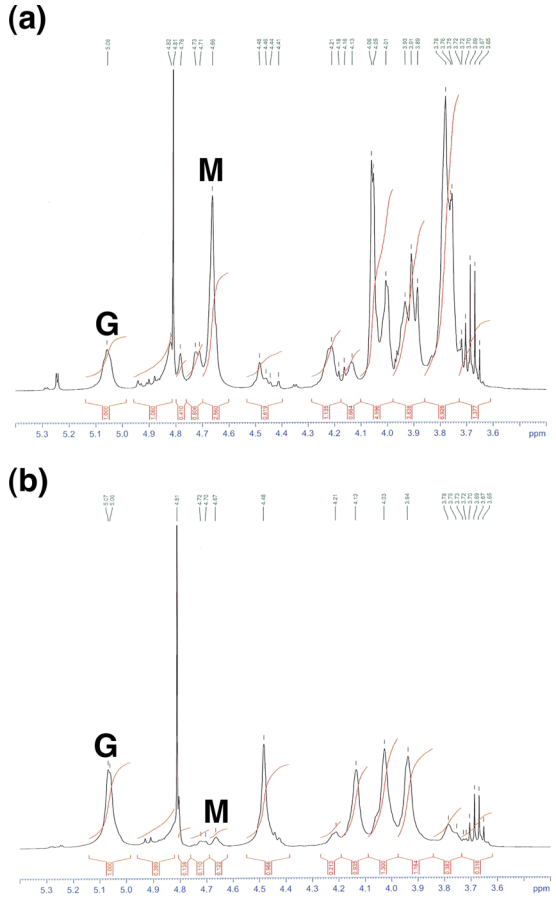

Figure 2. ^{1}H NMR spectra of (a) M-rich saccharides and (b) G-rich saccharides. Notations M and G indicate peaks derived from M and G residues, respectively.

were detected in the presence of 8 μM MMM, and the peak of the higher T_m intensified in the presence of 32 μM ligand (Figure 3, bottom). The decrease in the lower-T_m peak area and the increase in the higher-T_m peak area were dependent on ligand concentration. These features were also observed in AlgQ1 and AlgQ2 reaction mixtures that included GGG, ΔMMM, and ΔGGG (Figure 1 of the Supporting Information). When cellotriose was used as a ligand, a single lower T_m was obtained.

Because there are two forms (open and closed) of AlgQ1 and AlgQ2 upon substrate binding, low and high T_m values in the fluorescence profile of alginate-binding proteins appear to be derived from ligand-free (open) and ligand-bound (closed) forms, respectively. Thus, low and high T_m values were designated as T_{open} and T_{closed}, respectively. The presence of two T_m values was possibly caused by the difference in denaturation between ligand-free and -bound forms. The T_m profiles of AlgQ1 and AlgQ2 were distinct from those of *Campylobacter jejuni* cysteine-binding protein having a single T_m.[38] T_{open} and T_{closed} values calculated from the fluorescence profile of AlgQ1 and AlgQ2 in the absence and presence of the four ligands are listed in Table 1. The larger shift of T_{closed} was almost saturated at the ligand concentration of 512 μM. Because only a single T_m was detected in the denatured profile of AlgQ2 in the absence of ligand, T_{closed} of AlgQ2 could not be determined in the absence of ligand (Table 1). This indicates that AlgQ2 adopts only an open form in the absence of ligand. On the other hand, AlgQ1 gave two T_m values in the absence of

dx.doi.org/10.1021/bi300194f | *Biochemistry* 2012, 51, 3622−3633

Table 1. Temperature Denaturation Transitions of Open and Closed Forms

	MMM		GGG		ΔMMM		ΔGGG	
ligand (μM)	T_{open}	T_{closed}	T_{open}	T_{closed}	T_{open}	T_{closed}	T_{open}	T_{closed}
				AlgQ1				
0	51.32	55.52	50.98	55.26	51.35	55.05	50.88	54.98
1	51.05	55.88	51.35	55.57	51.07	56.55	50.81	55.63
2	50.85	56.24	50.85	55.29	51.53	57.61	51.52	55.99
4	51.43	56.46	50.95	55.46	53.59	59.46	51.65	56.54
8	52.5	57.56	50.54	56.45		61.62	52.88	57.63
16	53.47	58.42	51.44	56.54		63.86		58.87
32		59.58	52.43	58.13		65.41		59.64
64		61.59	53.41	58.82		66.36		61.49
128		63.53		61.04		68.08		62.92
256		64.25		61.51		68.95		64
512		65.9		63.38		70.41		65.07
				AlgQ2				
0	45.98		44.6		45.35		46.16	
1	45.18	51.51	45.26	51.44	44.72	53.57	45.01	54.05
2	45.84	51.46	44.55	51.47		54.64		55.04
4		52.91	45.38	51.53		56.46		57.94
8		53.97	46	51.99		58.69		59.04
16		55.72		53.3		59.91		60.58
32		57.1		54.86		61.05		61.53
64		58.48		56.56		62.68		62.84
128		59.46		58.07		63.53		63.66
256		60.95		59.03		64.55		63.52
512		61.85		60.36		65.65		63.77

ligand. AlgQ1 molecules even in the absence of ligand possibly contained the minor closed form as well as the major open form. The T_{open} values of AlgQ1 and AlgQ2 were almost constant in the presence of ligands at lower concentrations (<2 μM). This indicates that, in addition to ligand-bound AlgQ1 and AlgQ2 as a closed form, ligand-free proteins also existed as an open form in the presence of ligands. In the case of AlgQ1, T_{open} increased in proportion to ligand concentration at >4 μM. This increase in T_{open} was thought to be due to two possibilities: (i) the presence of a few ligand-bound AlgQ1 molecules still showing open-like form (the T_m of the ligand-bound AlgQ1 in the open-like form seems to increase in proportion to ligand concentration) and (ii) the interference effect of T_{closed} derived from an increased number of ligand-bound AlgQ1 molecules in a closed form on T_{open} for ligand-free and open form molecules (this interference is thought to be caused by the fluorescence detector).

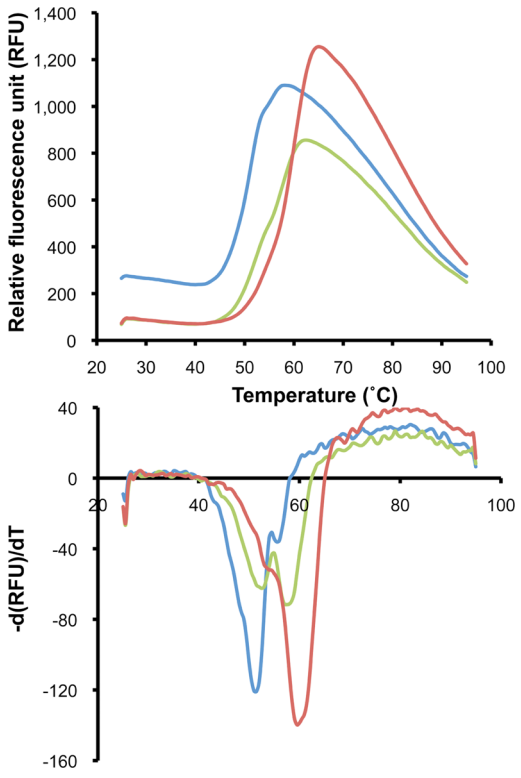

Figure 3. Analysis of substrate binding by DSF: (top) fluorescence profile of AlgQ1 with MMM (blue, 0 μM; green, 8 μM; red, 32 μM) and (bottom) negative derivative curve plot obtained from the fluorescence profile.

ΔT_{closed} (the difference in T_{closed} in the presence and absence of ligand) was dependent on ligand concentration, and all these oligosaccharides similarly induced the larger shift in T_{closed} (Figure 1 of the Supporting Information), suggesting that both binding proteins have a comparable affinity for alginate oligosaccharides with different M/G ratios. Thus, X-ray crystallography was performed to identify structural determinants in strain A1 solute-binding proteins with a broad substrate preference for both M and G.

Overall Structure. Crystal structures of strain A1 periplasmic alginate-binding proteins (AlgQ1 and AlgQ2) in complex with unsaturated alginate di- and tetrasaccharides (ΔMM and ΔMMGM) have already been determined, and the unsaturated residue at the nonreducing terminal saccharide of the substrate was strongly bound to the binding proteins at subsite 1.[17,18] The mode of binding of AlgQ1 to oligosaccharides with different M/G ratios was analyzed by X-ray crystallography. Four crystal structures of alginate-binding proteins in complex with oligosaccharides (AlgQ1-ΔMMM,

dx.doi.org/10.1021/bi300194f | Biochemistry 2012, 51, 3622−3633

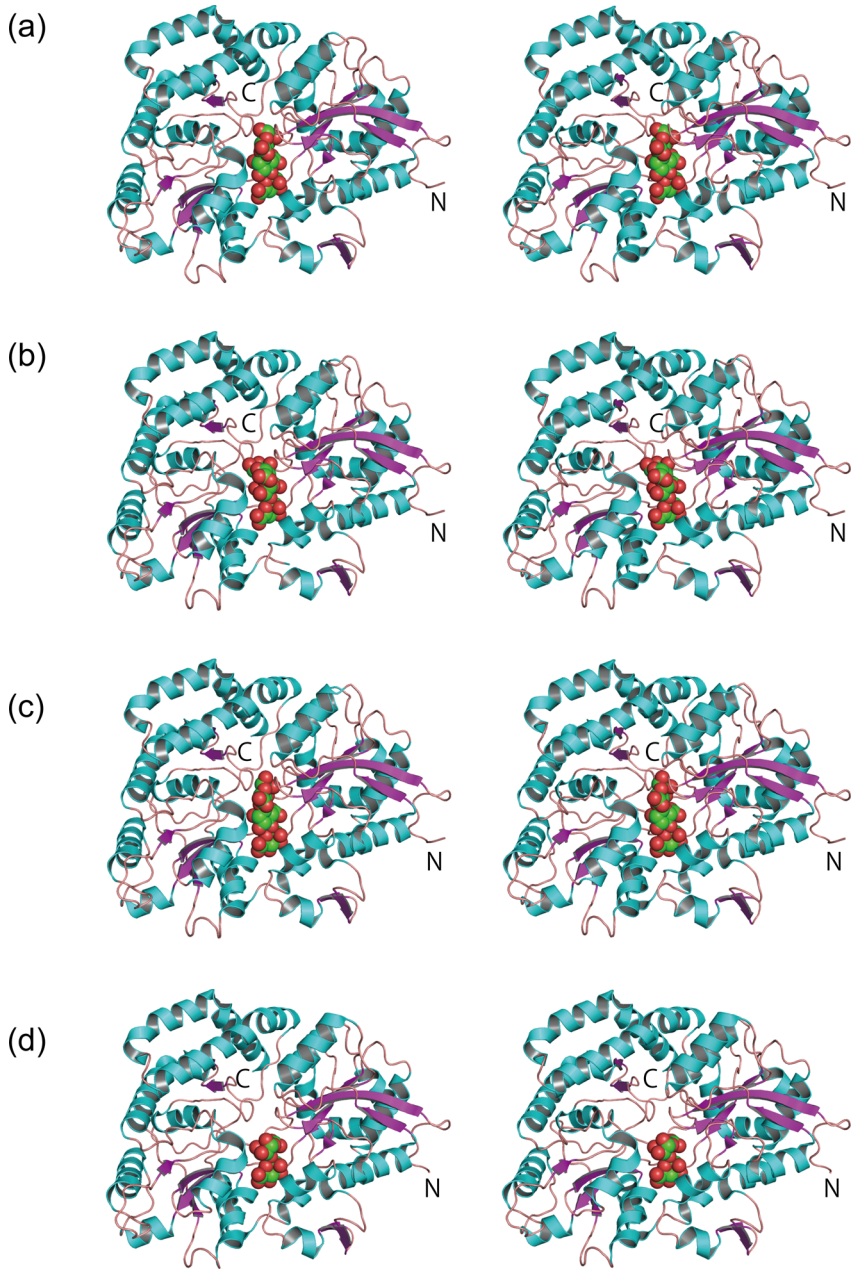

Figure 4. Overall structures of (a) AlgQ1-ΔMMM, (b) AlgQ1-ΔGGG, (c) AlgQ1-MMM, and (d) AlgQ1-MG complexes. Colors denote secondary structure elements (blue, α-helices; purple, β-strands; pink, loops and coils; sugar shown as a CPK model). N denotes the N-terminal end and C the C-terminal end.

AlgQ1-ΔGGG, AlgQ1-MMM, and AlgQ1-MG) were determined at 1.40, 1.50, 1.55, and 2.00 Å resolution, respectively (Figure 4). Statistics for data collection and structure refinement are summarized in Table 2. The polypeptide chain of AlgQ1 could be traced for almost all 490 amino acid residues, and the electron density of main and side chains was generally well-defined on the $2F_o - F_c$ map. A Ramachandran plot[39] revealed that almost all non-glycine residues lie within the most favored or additionally allowed regions. The residue (Lys-251) in the generously allowed region has been discussed previously.[17] In the AlgQ1-MG complex, two molecules designated A and B exist in the asymmetric unit, although only one molecule is in the asymmetric unit of the other three structures. The rmsd between molecules A and B in AlgQ1-MG is calculated to be 0.52, suggesting that the two molecules are structurally identical. The structure of molecule A was assessed later because molecules A and B are structurally identical to each other. Distinct from ligand-free binding proteins,[11] all molecules of AlgQ1 in these crystal structures show a closed form due to oligosaccharide binding. No significant difference was observed in overall structure among alginate oligosaccharide-bound AlgQ1 proteins.

Structure of Oligosaccharides. Alginate oligosaccharides in complex structures are bound to the deep cleft formed by the N- and C-terminal domains of AlgQ1. The composition and conformation of these oligosaccharides were analyzed on the basis of the $2F_o - F_c$ map (Figure 5). The oligosaccharides in AlgQ1-ΔMMM, AlgQ1-ΔGGG, and AlgQ1-MMM are defined as ΔM1-M2-M3, ΔG1-G2-G3, and M1-M2-M3, respectively. Sugar residue numbers corresponded to binding sites, namely

dx.doi.org/10.1021/bi300194f | *Biochemistry* 2012, 51, 3622−3633

Table 2. Data Collection and Refinement Statistics[a]

	AlgQ1-ΔMMM (PDB entry 3A09)	AlgQ1-ΔGGG (PDB entry 3VLV)	AlgQ1-MMM (PDB entry 3VLU)	AlgQ1-MG (PDB entry 3VLW)
		Crystal		
space group	$P2_1$	$P2_1$	$P2_1$	$P2_1$
cell dimensions				
a (Å)	58.4	58.4	58.5	79.8
b (Å)	67.7	67.5	67.5	67.5
c (Å)	63.2	61.6	61.7	90.7
β (deg)	95.0	94.6	94.6	93.3
no. of molecules per asymmetric unit	1	1	1	2
		Data Collection		
wavelength (Å)	1.0000	1.0000	1.0000	1.0000
resolution limit (last shell) (Å)	50.00−1.40 (1.45−1.40)[a]	50.00−1.50 (1.53−1.50)[a]	50.00−1.55 (1.58−1.55)[a]	50.00−2.00 (2.07−2.00)[a]
no. of measured reflections	333239	311011	282146	238701
no. of unique reflections	92768 (8095)	75638 (3550)	68880 (3488)	65158 (6439)
redundancy	3.6 (2.9)	4.1 (3.6)	4.1 (4.1)	3.7 (3.6)
R_{sym} (%)	4.7 (40.9)	4.9 (22.6)	6.8 (44.2)	9.4 (44.5)
$I/\sigma(I)$	27.3 (1.6)	45.9 (12.2)	40.2 (4.1)	20.4 (3.4)
completeness	95.5 (83.5)	99.3 (94.9)	99.6 (99.8)	99.8 (99.8)
Wilson plot *B* value	15.8	12.3	19.7	21.4
		Refinement		
resolution limit (Å)	50.00−1.40 (1.50−1.40)	50.00−1.50 (1.54−1.50)	50.00−1.55 (1.59−1.55)	50.00−2.00 (2.05−2.00)
R_{cryst} (%)	13.1 (28.2)	18.5 (24.6)	19.1 (26.6)	19.0 (23.0)
R_{free} (%)	20.8	20.4 (27.0)	21.3 (29.0)	22.3 (28.8)
no. of reflections used	87453	71833 (5041)	65278 (4568)	61732 (4566)
		Final Model		
no. of residues/no. of waters	490/766	490/819	490/524	489 × 2/458
no. of calcium ions	1	1	1	2
no. of saccharides	one trisaccharide	one trisaccharide	one trisaccharide	two disaccharides
no. of glycerols	0	0	0	18
average *B* factor				
protein	21.2	11.0	19.3	23.8
waters	36.7	25.9	30.8	32.3
saccharides	19.1	9.1	20.4	22.1
glycerols				45.8
rmsd from ideal				
bond lengths (Å)	0.012	0.006	0.006	0.006
bond angles	0.029 (Å)	0.932 (deg)	0.900 (deg)	0.949 (deg)
Ramachandran plot				
favored/allowed/outliers (%)	97.0/3.0/0	97.9/2.1/0	97.4/2.6/0	97.3/2.7/0
rotamer outliers (%)	4.3	1.3	2.0	2.9

[a]Data in the highest-resolution shells are given in parentheses.

subsites 1−3 in AlgQ1. Unexpectedly, in the case of AlgQ1 cocrystallized with disaccharide from G-rich saccharides, the binding protein accommodates MG, but not GG, in the active cleft. The M and G residues in MG are bound to AlgQ1 at subsites 1 and 2, respectively. The reason for the predominant accommodation of MG in AlgQ1 is described below.

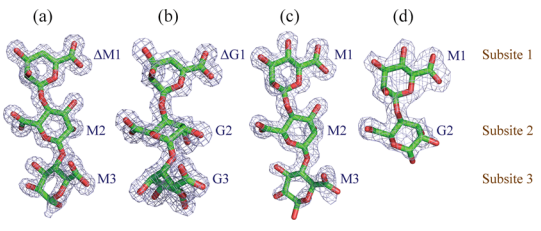

Figure 5. Structures of alginate oligosacchrides ($2F_o - F_c$ omit map; blue, contoured at 1.0σ): (a) ΔM1-M2-M3, (b) ΔG1-G2-G3, (c) M1-M2-M3, and (d) M1-G2. Carbons are colored green and oxygens red.

A structural difference exists at the nonreducing terminal residue between saturated and unsaturated saccharides. The nonreducing terminal residue of unsaturated saccharides contains no hydroxyl group at C4 because the double bond forms between C4 and C5 of the residue through the *β*-elimination reaction, i.e., lyase catalysis.[13] Because of the arrangement of C3−C6 atoms in one plane, the unsaturated residue shows a partial planar ring structure. ΔM and ΔG are structurally identical for the following two reasons: (i) M and G are mutually C5 epimers, and (ii) the unsaturated sugar residue lacks the hydrogen atom of C5.

Because saccharides with a pyranose ring show different configurations, the conformation of alginate oligosaccharides in complex structures was analyzed. On the basis of the electron density map of sugar residues, the saturated M and G residues

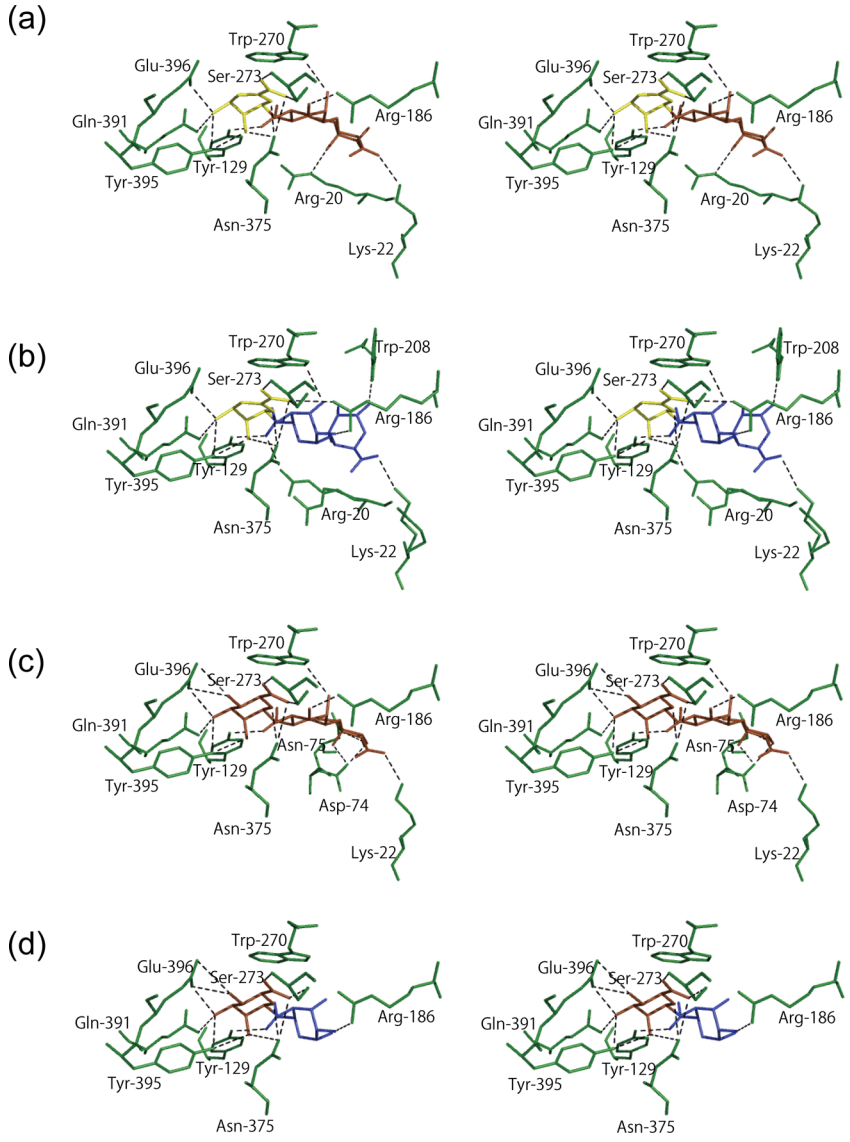

Figure 6. Alginate-binding site (stereoviews). Residues colored green bind to oligosaccharides through hydrogen bonds (dashed lines). Interactions between AlgQ1 and oligosaccharides are shown as a stick model (blue, G; brown, M; yellow, ΔM and ΔG): (a) ΔM1-M2-M3, (b) ΔG1-G2-G3, (c) M1-M2-M3, and (d) M1-G2.

were found to adopt $^4C_1$ and $^1C_4$ chair configurations, respectively, indicating that the sequence of M residues shows a flat chain conformation in parallel with glycosidic bonds, whereas a buckled structure is constructed by the sequence of G residues. This structural feature of oligosaccharides coincides with that of well-characterized M- and G-rich blocks.[1,40] Therefore, ΔMMM and MMM bound to AlgQ1 form a linear extended conformation in contrast to GGG.

Interactions between the Binding Protein and Oligosaccharides. Alginate oligosaccharides are bound to AlgQ1 by hydrogen bonds and van der Waals (C−C) contacts (Figure 6). Hydrogen bonds formed between AlgQ1 and oligosaccharide molecules are listed in Table 3. The crystal structure of the AlgQ1-ΔMMM complex reveals that the number of direct hydrogen bonds is 14 (ΔM1, 9; ΔM2, 3; ΔM3, 2) and the number of water-associated hydrogen bonds is 10 (ΔM1, 2; ΔM2, 5; ΔM3, 3). In the AlgQ1-ΔGGG complex, the number of direct hydrogen bonds is 16 (ΔG1, 10; ΔG2, 4; ΔG3, 2) and the number of water-associated hydrogen bonds is 16 (ΔG1, 2; ΔG2, 7; ΔG3, 7). Between AlgQ1 and MMM, the number of direct hydrogen bonds is 18 (M1, 11; M2, 3; M3, 4) and the number of water-associated hydrogen bonds is 13 (M1, 3; M2, 6; M3, 4). Between AlgQ1 and MG, the number of direct hydrogen bonds is 13 (M1, 11; G2, 2) and the number of water-associated hydrogen bonds is 7 (M1, 3; G2, 4).

The C−C contacts between AlgQ1 and oligosaccharide molecules are summarized in Table 4. A slight difference is observed in the contacts at subsite 1 between AlgQ1 in complex with saturated and unsaturated oligosaccharides. The C4 atom of unsaturated residues in ΔMMM and ΔGGG is closer to Trp-270 than that of saturated residues in MMM and MG (Figure 6a). This is due to the different ring structures of saturated (chair configuration) and unsaturated (partial planar configuration) residues. Similar to previously determined structures of binding proteins in complex with unsaturated oligosaccharides,[17,18] AlgQ1 shows a strong stacking interaction with saturated and unsaturated nonreducing terminal residues of substrates.

dx.doi.org/10.1021/bi300194f | *Biochemistry* 2012, 51, 3622−3633

Table 3. Interactions between AlgQ1 and Oligosaccharides

	protein/water		AlgQ1-ΔMMM	AlgQ1-ΔGGG	AlgQ1-MMM	AlgQ1-MG
sugar atom	subsite 1	atom	ΔM1	ΔG1	M1	M1
O2	Asn-375	ND2	3.0	3.2	(3.3)[a]	(3.2)[a]
O2	Tyr-395	OH	3.1	3.1	3.1	3.2
O2	water		2.8	2.8	2.9	2.9
O3	Glu-396	OE1	2.6	2.6	2.7	2.7
O3	Tyr-395	OH	2.8	2.8	2.7	2.7
O3	Gln-391	NE2	3.2	(3.3)[a]	3.1	3.1
O4	Glu-396	OE1	–	–	3.2	3.2
O4	Glu-396	OE2	–	–	3.1	3.1
O4	water		–	–	3.0	3.0
O5	Asn-375	ND2	3.0	3.0	3.1	3.0
O61	Arg-186	NH2	–	3.2	–	–
O61	Asn-375	ND2	3.0	(3.3)[a]	3.0	3.0
O61	Ser-273	OG	2.6	2.6	2.6	2.7
O62	Ser-273	N	2.9	3.1	3.0	3.0
O62	water		2.7	2.8	2.9	2.8
	protein/water		AlgQ1-ΔMMM	AlgQ1-ΔGGG	AlgQ1-MMM	AlgQ1-MG
sugar atom	subsite 2	atom	M2	G2	M2	G2
O2	Arg-186	NH1	–	3.0	–	2.7
O2	Trp-270	NE1	3.1	–	3.0	–
O2	water		2.7	2.7	2.7	–
O2	water		2.6	3.1	2.9	–
O3	Arg-186	NH1	–	–	2.9	–
O3	Arg-186	NH2	2.8	–	–	–
O3	Trp-270	NE1	–	3.1	–	–
O3	water		–	2.8	–	2.6
O3	water		–	3.0	–	–
O4	water		3.0	3.1	3.1	–
O61	Arg-20	NH2	–	3.0	–	–
O61	Tyr-129	OH	2.6	2.7	2.7	2.7
O61	water		2.7	2.8	2.7	2.7
O62	water		2.7	2.7	2.7	2.7
O62	water		–	–	2.8	2.7
	protein/water		AlgQ1-ΔMMM	AlgQ1-ΔGGG	AlgQ1-MMM	
sugar atom	subsite 3	atom	M3	G3	M3	
O1	Asp-74	OD2	–	–	2.6	
O1	Asn-75	ND2	–	–	3.2	
O1	Trp-208	NE1	–	2.7	–	
O1	water		2.9	2.8	–	
O2	Arg-20	NE	3.1	–	–	
O2	Asp-74	OD2	–	–	2.9	
O2	water		2.7	2.6	2.9	
O2	water		–	2.9	–	
O3	water		2.9	2.8	2.9	
O3	water		–	2.7	–	
O4	water		–	3.2	3.1	
O4	water		–	–	3.0	
O62	Lys-22	NZ	2.8	2.8	2.8	
O62	water		–	2.7	–	

[a]Although lengths of hydrogen bonds listed here are <3.2 Å, the values of >3.2 Å are presented in parentheses when no significant conformational differences are observed among determined structures.

Binding Mode at Subsite 1. Because the intrinsic substrate for macromolecule import in strain A1 cells is an alginate polysaccharide with a saturated residue at nonreducing terminal saccharides, but not unsaturated saccharides, the interaction at subsite 1 between AlgQ1 and MMM was focused (Tables 3 and 4, Figure 6c, and Figure 2a of the Supporting Information). Distinct from the unsaturated M residue (ΔM1), the saturated M1 residue has a hydroxyl group at C4. The O4 atom at this hydroxyl group of the M1 residue forms two hydrogen bonds with the carboxyl group of Glu-396. Furthermore, the O4 atom of the M1 residue indirectly interacts with Ala-272 and Glu-396 through a water molecule, although this water molecule also exists in complex structures of AlgQ1-MG, AlgQ1-ΔMMM, and AlgQ1-ΔGGG.

To clarify the mode of binding of AlgQ1 to the saturated G residue at subsite 1, the disaccharide was prepared from G-rich saccharides. Although the content of G residues in G-rich saccharides was determined to be >90% by NMR (Figure 2), the disaccharide in complex with AlgQ1 in the crystal structure was found to be MG, not GG. Because MG is considered to be a minor component in hydrolysates from G-rich saccharides in comparison with GG, AlgQ1 seems to prefer the M residue at subsite 1 rather than the G residue. The carboxyl group of the M1 residue in AlgQ1-MG and AlgQ1-MMM is bound to Ser-273 through formation of two hydrogen bonds (Table 3, Figure 6c,d, and Figure 2a of the Supporting Information). Moreover, the aromatic Trp-270 residue exhibits a stacking interaction with the M1 residue at subsite 1. There is a difference in orientation of the carboxyl group between M and G residues because both are C5 epimers. Although the interaction at subsite 1 between the saturated G residue and AlgQ1 was simulated, no saturated G residue can be accommodated at subsite 1 because of steric hindrance. The arrangement of amino acid residues at subsite 1 of AlgQ1 is almost identical to that of AlgQ2, suggesting that both strain A1 alginate-binding proteins can interact with only alginate molecules with the saturated M residue at the nonreducing terminus. This preference can be explained with the reason stated below. In the production of both alginates by bacteria and seaweeds, the mannuronan polymer is first synthesized as a precursor, and some M residues in the precursor are then epimerized to G residues by mannuronan C5-epimerases. Several epimerases from the alginate-producing bacterium *Azotobacter vinelandii* have already been characterized, and these enzymes are shown not to act on nonreducing terminal saccahrides.[41,42] Seaweed, *Laminaria digitata* expresses several genes sharing significant similarities with bacterial epimerases,[7] suggesting that no conversion of an M residue to a G residue at the nonreducing terminal saccharide occurs in seaweed alginate. Therefore, the nonreducing terminal saccharide of bacterial and seaweed alginate is essentially the M residue, and the strain A1 alginate-binding proteins AlgQ1 and AlgQ2 accommodate only the M residue at subsite 1.

Flexible Accommodation at Subsites 2 and 3. Distinct from subsite 1, both M and G residues are accommodated at subsites 2 and 3 (Figures 5 and 6). Structural comparison was performed for interactions at subsites 2 and 3 between AlgQ1-ΔMMM and AlgQ1-ΔGGG or between AlgQ1-MMM and AlgQ1-MG (Tables 3 and 4, Figure 7, and Figure 2 of the Supporting Information). At subsite 2, hydrogen bonds are formed in AlgQ1-ΔMMM and AlgQ1-MMM between Trp-270 and the O2 atom of the hydroxyl group of the M2 residue and between Arg-186 and the O3 atom of the hydroxyl group of the M2 residue. On the other hand, interactions in AlgQ1-ΔGGG and/or AlgQ1-MG occur via formation of a hydrogen bond

dx.doi.org/10.1021/bi300194f | *Biochemistry* 2012, 51, 3622−3633

Table 4. C−C Contacts between Alginate-Binding Proteins and Alginate Oligosaccharides[a]

			no. of contacts			
	bond atom		AlgQ1-ΔMMM	AlgQ1-ΔGGG	AlgQ1-MMM	AlgQ1-MG
sugar atom	subsite S1	element/domain	ΔM1	ΔG1	M1	M1
C1	Trp-270	SC2/C	7	7	6	6
C2	Trp-270	SC2/C	1	1		
C3	Trp-270	SC2/C	2	2	2	2
C3	Glu-396	H19/N	1	1	1	1
C4	Trp-270	SC2/C	3	3		1
C4	Asn-375	H18/N			1	1
C4	Glu-396	H19/N	1	1		1
C4	Trp-399	L-H19:H20/N-C	1	1	2	2
C5	Trp-270	SC2/C	5	4	5	5
C5	Asn-375	H18/N	1	1		
C5	Trp-399	L-H19:H20/N-C		1		
C6	Trp-270	SC2/C	4	4	3	3
C6	Ser-273	H14/C	1	1	1	1
C6	Asn-375	H18/N	1	1	1	1
C6	Trp-399	L-H19:H20/N-C	1	1	1	1
			no. of contacts			
	bond atom		AlgQ1-ΔMMM	AlgQ1-ΔGGG	AlgQ1-MMM	AlgQ1-MG
sugar atom	subsite S2	element/domain	M2	G2	M2	G2
C1	Arg-20	L-SA5:SA6/N		1		2
C2	Arg-186	L-SC1:H9/C	1		1	1
C3	Arg-186	L-SC1:H9/C				1
C3	Trp-270	SC2/C	1	3	1	2
C4	Trp-270	SC2/C	3	4	2	4
C5	Arg-20	L-SA5:SA6/N			1	
C5	Trp-270	SC2/C		1		
C6	Tyr-129	SA1/C	2	2	2	2
C6	Trp-270	SC2/C	1	1	1	1
			no. of contacts			
	bond atom		AlgQ1-ΔMMM	AlgQ1-ΔGGG	AlgQ1-MMM	
sugar atom	subsite S3	element/domain	M3	G3	M3	
C1	Arg-20	L-SA5:SA6/N	2		1	
C1	Arg-74	SA4/N	1			
C1	Asp-187	L-SC1:H9/C		1		
C2	Arg-20	L-SA5:SA6/N	1		1	
C2	Arg-74	SA4/N	2			
C3	Arg-20	L-SA5:SA6/N		1		
C3	Arg-313	L-SC4:SA3/C−N				
C4	Arg-20	L-SA5:SA6/N	2	5	2	
C5	Arg-20	L-SA5:SA6/N	2	6	2	
C6	Arg-20	L-SA5:SA6/N	3	6	3	

[a]Distance of ≤4.4 Å.

between Trp-270 and the O3 atom of the hydroxyl group of the G2 residue and between Arg-186 and the O2 atom of the hydroxyl group of the G2 residue. In contrast, the O61 and O62 atoms of carboxyl groups of both M2 and G2 residues are commonly recognized by Tyr-129. There is little significant difference in C−C contacts at subsite 2 between the modes of binding of AlgQ1 to M and G residues. Moreover, at subsite 3, the O62 atoms of carboxyl groups of both M3 and G3 residues are commonly hydrogen-bonded to Lys-22, although few direct interactions are observed between AlgQ1 and oligosaccharides.

Tyr-129 interacts with the carboxyl groups of both M2 and G2 residues bound at subsite 2, while Trp-270 and Arg-186 recognize their different hydroxyl groups. At subsite 3, Lys-22 binds carboxyl groups of both M3 and G3 residues. On the basis of these results, substrate carboxyl groups are found to be recognized by specific residues Tyr-129 at subsite 2 and Lys-22 at subsite 3. The O2 atom of residue M2 and the O3 atom of residue G2 are located at almost the same position and, therefore, are recognized by residues such as Trp-270 at subsite 2. In other words, AlgQ1 strictly recognizes substrate carboxyl groups by specific residues but interacts appropriately with substrate hydroxyl groups. These structural characteristics at the binding site are probably involved in the flexible accommodation of residues M and G at subsites 2 and 3.

CONCLUSIONS

The strain A1 periplasmic solute-binding proteins AlgQ1 and AlgQ2 strictly recognize the nonreducing saturated M residue

dx.doi.org/10.1021/bi300194f | Biochemistry 2012, 51, 3622−3633

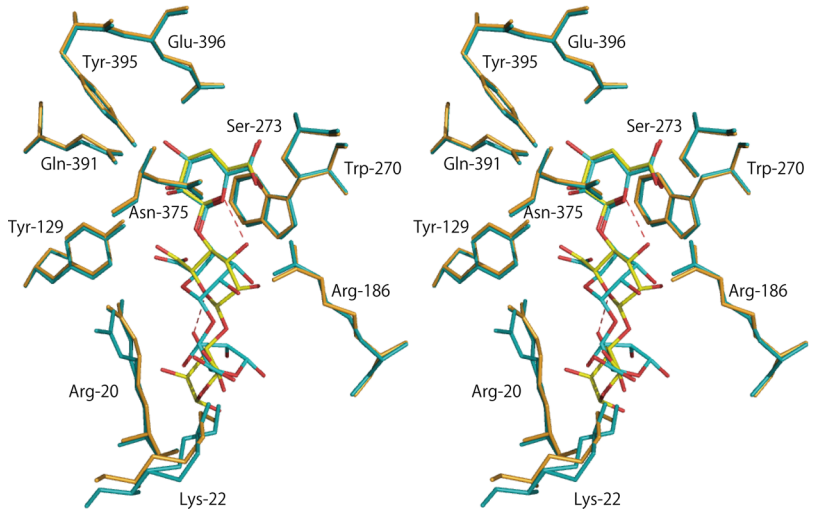

Figure 7. Superposition of AlgQ1 with bound ΔMMM and ΔGGG: yellow, AlgQ1-ΔMMM; cyan, AlgQ1-ΔGGG. Oxygen atoms of sugar residues are colored in red. Hydrogen bonds formed between sugar residues are represented as dashed lines. These two intrasugar hydrogen bonds are formed in ΔMMM but not in ΔGGG. Although conformations of ΔMMM and ΔGGG are apparently different, both bind in the same position of AlgQ1 without a significant change in the structure of the protein.

of substantial substrate alginate at subsite 1. These proteins interact appropriately with substrate hydroxyl groups at subsites 2 and 3 to accommodate the M or G residue, while substrate carboxyl groups are strictly recognized by specific residues. This mechanism of substrate recognition allows AlgQ1 and AlgQ2 to exhibit the binding ability with heteropolysaccharide alginate, leading to the sufficient growth of strain A1 cells in various alginates with different M/G ratios.

■ ASSOCIATED CONTENT

Supporting Information

AlgQ1 and AlgQ2 were subjected to a substrate binding assay using various alginate oligosaccharides through DSF analysis (Figure 1), and modes of binding at each subsite were compared using AlgQ1 in complex with various alginate oligosaccharides (Figure 2). This material is available free of charge via the Internet at http://pubs.acs.org.

■ AUTHOR INFORMATION

Corresponding Author

*Laboratory of Basic and Applied Molecular Biotechnology, Graduate School of Agriculture, Kyoto University, Uji, Kyoto 611-0011, Japan. E-mail: kmurata@kais.kyoto-u.ac.jp. Telephone: +81-774-38-3766. Fax: +81-774-38-3767.

Funding

This work was supported in part by Grants-in-Aid from the Japan Society for the Promotion of Science (K.M. and W.H.) and by the Targeted Proteins Research Program (W.H.) of the Ministry of Education, Culture, Sports, Science and Technology (MEXT) of Japan.

Notes

The authors declare no competing financial interest.

■ ACKNOWLEDGMENTS

We thank Drs. S. Baba and N. Mizuno of the Japan Synchrotron Radiation Research Institute (JASRI) for their kind help in data collection. Diffraction data for crystals were collected at the BL-38B1 station of SPring-8 with the approval (2011A1186 and 2008B1191) of JASRI. We also thank Ms. Ai Matsunami and Ms. Chizuru Tokunaga for their excellent technical assistance.

■ ABBREVIATIONS

M, β-D-mannuronate; G, α-L-guluronate; strain A1, *Sphingomonas* sp. A1; ABC, ATP-binding cassette; NMR, nuclear magnetic resonance; DSF, differential scanning fluorimetry; T_m, melting temperature.

■ REFERENCES

(1) Gacesa, P. (1988) Alginates. *Carbohydr. Polym. 8*, 161−182.
(2) Remminghorst, U., and Rehm, B. H. (2006) Bacterial alginates: From biosynthesis to applications. *Biotechnol. Lett. 28*, 1701−1712.
(3) Akiyama, H., Endo, T., Nakakita, R., Murata, K., Yonemoto, Y., and Okayama, K. (1992) Effect of depolymerized alginates on the growth of bifidobacteria. *Biosci., Biotechnol., Biochem. 56*, 355−356.
(4) May, T. B., and Chakrabarty, A. M. (1994) *Pseudomonas aeruginosa*: Genes and enzymes of alginate synthesis. *Trends Microbiol. 2*, 151−157.
(5) Wong, T. Y., Preston, L. A., and Schiller, N. L. (2000) Alginate lyase: Review of major sources and enzyme characteristics, structure-function analysis, biological roles, and applications. *Annu. Rev. Microbiol. 54*, 289−340.
(6) Singh, A., Nigam, P. S., and Murphy, J. D. (2011) Renewable fuels from algae: An answer to debatable land based fuels. *Bioresour. Technol. 102*, 10−16.
(7) Nyvall, P., Corre, E., Boisset, C., Barbeyron, T., Rousvoal, S., Scornet, D., Kloareg, B., and Boyen, C. (2003) Characterization of mannuronan C-5-epimerase genes from the brown alga *Laminaria digitata*. *Plant Physiol. 133*, 726−735.
(8) Garron, M. L., and Cygler, M. (2010) Structural and mechanistic classification of uronic acid-containing polysaccharide lyases. *Glycobiology 20*, 1547−1573.
(9) Murata, K., Kawai, S., Mikami, B., and Hashimoto, W. (2008) Superchannel of bacteria: Biological significance and new horizons. *Biosci., Biotechnol., Biochem. 72*, 265−277.
(10) Hisano, T., Kimura, N., Hashimoto, W., and Murata, K. (1996) Pit structure on bacterial cell surface. *Biochem. Biophys. Res. Commun. 220*, 979−982.
(11) Momma, K., Mikami, B., Mishima, Y., Hashimoto, W., and Murata, K. (2002) Crystal structure of AlgQ2, a macromolecule (alginate)-binding protein of *Sphingomonas* sp. A1 at 2.0 Å resolution. *J. Mol. Biol. 316*, 1061−1069.

(12) Momma, K., Okamoto, M., Mishima, Y., Mori, S., Hashimoto, W., and Murata, K. (2000) A novel bacterial ATP-binding cassette (ABC) transporter system that allows uptake of macromolecules. *J. Bacteriol. 182*, 3998−4004.
(13) Yoon, H.-J., Hashimoto, W., Miyake, O., Okamoto, M., Mikami, B., and Murata, K. (2000) Overexpression in *Escherichia coli*, purification, and characterization of *Sphingomonas* sp. A1 alginate lyases. *Protein Expression Purif. 19*, 84−90.
(14) Hashimoto, W., Miyake, O., Momma, K., Kawai, S., and Murata, K. (2000) Molecular identification of oligoalginate lyase of *Sphingomonas* sp. strain A1 as one of the enzymes required for complete depolymerization of alginate. *J. Bacteriol. 182*, 4572−4577.
(15) Eitinger, T., Rodionov, D. A., Grote, M., and Schneider, E. (2011) Canonical and ECF-type ATP-binding cassette importers in prokaryotes: Diversity in modular organization and cellular functions. *FEMS Microbiol. Rev. 35*, 3−67.
(16) Hugouvieux-Cotte-Pattat, N., and Reverchon, S. (2001) Two transporters, TogT and TogMNAB, are responsible for oligogalacturonide uptake in *Erwinia chrysanthemi* 3937. *Mol. Microbiol. 41*, 1125−1132.
(17) Momma, K., Mishima, Y., Hashimoto, W., Mikami, B., and Murata, K. (2005) Direct evidence for *Sphingomonas* sp. A1 periplasmic proteins as macromolecule-binding proteins associated with ABC transporter: Molecular insights into alginate transport in the periplasm. *Biochemistry 44*, 5053−5064.
(18) Mishima, Y., Momma, K., Hashimoto, W., Mikami, B., and Murata, K. (2003) Crystal structure of AlgQ2, a macromolecule (alginate)-binding protein of *Sphingomonas* sp. A1, complexed with an alginate tetrasaccharide at 1.6-Å resolution. *J. Biol. Chem. 278*, 6552−6559.
(19) Takeda, H., Yoneyama, F., Kawai, S., Hashimoto, W., and Murata, K. (2011) Bioethanol production from marine biomass alginate by metabolically engineered bacteria. *Energy Environ. Sci. 4*, 2575−2581.
(20) Sambrook, J., Fritsch, E. F., and Maniatis, T. (1989) *Molecular cloning: A laboratory manual*, Cold Spring Harbor Laboratory Press, Plainview, NY.
(21) Laemmli, U. K. (1970) Cleavage of structural proteins during the assembly of the head of bacteriophage T4. *Nature 227*, 680−685.
(22) Haug, A., Larsen, B., and Smidsrod, O. (1966) A study of the constitution of alginic acid by partial acid hydrolysis. *Acta Chem. Scand. 20*, 183−190.
(23) Miyake, O., Ochiai, A., Hashimoto, W., and Murata, K. (2004) Origin and diversity of alginate lyases of families PL-5 and -7 in *Sphingomonas* sp. strain A1. *J. Bacteriol. 186*, 2891−2896.
(24) Miller, G. L. (1959) Use of dinitrosalicylic acid reagent for determination of reducing sugar. *Anal. Chem. 31*, 426−428.
(25) Niesen, F. H., Berglund, H., and Vedadi, M. (2007) The use of differential scanning fluorimetry to detect ligand interactions that promote protein stability. *Nat. Protoc. 2*, 2212−2221.
(26) Otwinowski, Z., and Minor, W. (1997) Processing of X-ray diffraction data collected in oscillation mode. *Methods Enzymol. 276*, 307−326.
(27) Brünger, A. T., Adams, P. D., Clore, G. M., DeLano, W. L., Gros, P., Grosse-Kunstleve, R. W., Jiang, J. S., Kuszewski, J., Nilges, M., Pannu, N. S., Read, R. J., Rice, L. M., Simonson, T., and Warren, G. L. (1998) Crystallography and NMR system (CNS): A new software system for macromolecular structure determination. *Acta Crystallogr. D54*, 905−921.
(28) Sheldrick, G. M. (2008) A short history of SHELX. *Acta Crystallogr. D64*, 112−122.
(29) Vagin, A., and Teplyakov, A. (1997) MOLREP: An automated program for molecular replacement. *J. Appl. Crystallogr. 30*, 1022−1025.
(30) Collaborative Computational Project, Number 4 (1994) The CCP4 suite: Programs for protein crystallography. *Acta Crystallogr. D50*, 760−763.
(31) Murshudov, G. N., Vagin, A. A., and Dodson, E. J. (1997) Refinement of macromolecular structures by the maximum-likelihood method. *Acta Crystallogr. D53*, 240−255.
(32) Emsley, P., and Cowtan, K. (2004) Coot: Model-building tools for molecular graphics. *Acta Crystallogr. D60*, 2126−2132.
(33) Schuettelkopf, A. W., and Van Aalten, D. M. F. (2004) PRODRG: A tool for high-throughput crystallography of protein-ligand complexes. *Acta Crystallogr. D60*, 1355−1363.
(34) Kabsch, W. (1976) A solution for the best rotation to relate two sets of vectors. *Acta Crystallogr. A32*, 922−923.
(35) Laskowski, R. A., MacArthur, M. W., Moss, D. S., and Thornton, J. M. (1993) PROCHECK: A program to check the stereochemical quality of protein structures. *J. Appl. Crystallogr. 26*, 283−291.
(36) DeLano, W. L. (2004) *The PyMOL Molecular Graphics System*, DeLano Scientific LLC, San Carlos, CA.
(37) Berman, H. M., Westbrook, J., Feng, Z., Gilliland, G., Bhat, T. N., Weissig, H., Shindyalov, I. N., and Bourne, P. E. (2000) The protein data bank. *Nucleic Acids Res. 28*, 235−242.
(38) Giuliani, S. E., Frank, A. M., and Collart, F. R. (2008) Functional assignment of solute-binding proteins of ABC transporters using a fluorescence-based thermal shift assay. *Biochemistry 47*, 13974−13984.
(39) Ramachandran, G. N., and Sasisekharan, V. (1968) Conformations of polypeptides and proteins. *Adv. Protein Chem. 23*, 283−438.
(40) Llanes, F., Ryan, D. H., and Marchessault, R. H. (2000) Magnetic nanostructured composites using alginates of different M/G ratios as polymeric matrix. *Int. J. Biol. Macromol. 27*, 35−40.
(41) Holtan, S., Bruheim, P., and Skjåk-Bræk, G. (2006) Mode of action and subsite studies of guluronan block-forming mannuronan C-5 epimerases AlgE1 and AlgE6. *Biochem. J. 395*, 319−329.
(42) Campa, C., Holtan, S., Nilsen, N., Bjerkan, T. M., Stokke, B. T., and Skjåk-Bræk, G. (2004) Biochemical analysis of the processive mechanism for epimerization of alginate by mannuronan C-5 epimerase AlgE4. *Biochem. J. 381*, 155−164.